

Synthesis and Structure of Mercurous Ion and Dinuclear Lead(II) Complexes of the 28-Membered Selenaza Macrocycle: Dominance of the Chelate Ring Size Effect and Conformational Requirement over Soft–Soft Interactions

Snigdha Panda,[†] Harkesh B. Singh,^{*,†} and Ray J. Butcher[‡]

Departments of Chemistry, Indian Institute of Technology, Bombay, Powai, Mumbai 400076, India, and Howard University, Washington, DC 20059

Received October 16, 2003

The flexible and larger ring size macrocycle **4** (C₃₆H₄₆N₆Se₂) afforded stable complex **5** [Hg₂(PF₆)₂{C₃₆H₄₆N₆Se₂}] on treatment with 1 equiv of mercuric acetate followed by addition of NH₄PF₆. The reaction of Pb(OCOCH₃)₂·4H₂O with **4** followed by treatment with NH₄PF₆ resulted in a dinuclear lead complex (**6**) [Pb₂(PF₆)₂(OCOCH₃)₂{C₃₆H₄₆N₆Se₂}]. The crystal structures of complexes **5** and **6** are described: C₃₆H₄₆F₁₂Hg₂N₆P₂Se₂ *a* = 9.5106(5) Å, *b* = 11.5222(6) Å, *c* = 11.8161(6) Å, α = 115.6110(10)°, β = 96.5190(10)°, γ = 106.2910(10)°, monoclinic, *P*1̄, *Z* = 1; C₄₄H₅₇F₁₂N₈O₄P₂Pb₂Se₂ *a* = 9.4668(5) Å, *b* = 11.9937(6) Å, *c* = 25.2319(14) Å, α = 102.4130(10)°, β = 97.6130(10)°, γ = 94.8540(10)°, monoclinic, *P*1̄, *Z* = 2. The crystal structure of **5** revealed that Hg₂²⁺ is trapped inside the cavity of the macrocycle. The geometry around the mercurous ion is antiprismatic with Hg₂²⁺ coordinating to six nitrogen atoms forming four five-membered rings, and there is no interaction between the mercurous ion and the selenium donor atoms. The single crystal X-ray crystal structure of **6** indicates a distorted octahedral geometry around each lead atom in the cavity of the macrocycle due to presence of the stereochemically active lone pair on Pb(II). The octahedral geometry around each Pb(II) is satisfied by coordination to 3 nitrogen atoms, two oxygen atoms of the chelating acetate group, and bridging of one of the oxygen atoms of the nearby acetate.

Introduction

Macrocyclic ligands have been attracting much interest owing to their exceptional complexation potential which has facilitated the study of metals in unusual circumstances, e.g., uncommon coordination numbers, coordination geometries, donor atoms, or oxidation states.¹ Over recent years, considerable effort has been directed toward the design and synthesis of new mixed donor selenoether/telluroether macrocyclic ligands in order to investigate their ligation properties toward transition and post-transition metal cations.² Recently, the study of coordination chemistry of Hg(II) and

Pb(II) has been of crucial importance due to the problem of environmental contamination by these heavy metals.³ Hg(II) is a soft Lewis acid, and Pb(II) is considered to be an intermediate acid and expected to bind to a broad range of donor atoms. Hence, selenoethers, both homo and mixed donors containing soft Se and hard O/N, can be effective chelating agents for these cations.

As part of our research on the complexation properties of mixed donor chalcogenaaza macrocycles, we have recently reported the synthesis of novel Schiff base chalcogenaaza (Se, Te) macrocycles of various ring sizes **1–3** and studied

* To whom correspondence should be addressed. E-mail: chhbsia@chem.iitb.ac.in.

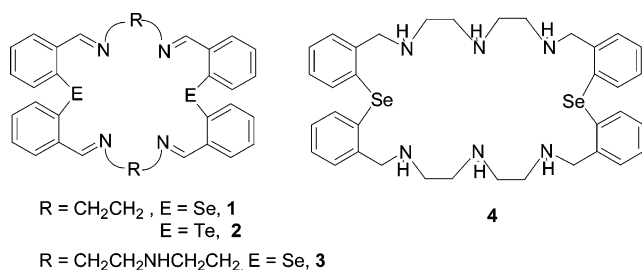
[†] Indian Institute of Technology.

[‡] Howard University.

- (1) (a) Lindoy, L. F. In *The Chemistry of Macrocyclic Ligand Complexes*; Cambridge University Press: Cambridge, U.K., 1989. (b) Dietrich, B.; Viout, P.; Lehn, J.-M. *Macrocyclic Chemistry: Aspects of Organic and Inorganic Supramolecular Chemistry*; VCH: Weinheim, 1993. (c) Lehn, J.-M. *Supramolecular Chemistry: Concepts and Perspectives*; VCH: Weinheim, 1995. (d) Dodziuk, H. *Introduction to Supramolecular Chemistry*; Kluwer Academic: Dordrecht, 2002.

- (2) (a) Hope, E. G.; Levason, W. *Coord. Chem. Rev.* **1993**, *122*, 109 and references therein. (b) Levason, W.; Orchard, S. D.; Reid, G. *Coord. Chem. Rev.* **2002**, *225*, 159 and references therein. (c) Singh, A. K.; Sharma, S. *Coord. Chem. Rev.* **2000**, *209*, 49 and references therein. (d) Bhula, R.; Arnold, A. P.; Jackson, W. G. *Chem. Commun.* **1996**, 143. (e) Levason, W.; Matthews, M. L.; Patel, R.; Reid, G.; Webster, M. *New J. Chem.* **2003**, *27*, 1784. (f) Levason, W.; Reid, G. *Compr. Coord. Chem. II* **2004**, *1*, 399 and references therein. (3) Aragoni, M. C.; Arca, M.; Demartin, F.; Devillanova, F. A.; Isaia, F.; Garau, A.; Lippolis, V.; Jalali, F.; Papke, U.; Shamsipur, M.; Tei, L.; Yari, A.; Verani, G. *Inorg. Chem.* **2002**, *41*, 6623 and references therein.

their complexation toward various transition metal ions.^{4–10} However, these Schiff base macrocycles were found to be prone to transmetalation and hydrolysis on treatment with metal salts leading to cleavage of the macrocycle. The selenaza Schiff base macrocycle **1** forms hydrolyzed product with Pd(II) cation⁹ whereas the telluraza Schiff base macrocycle **2** forms transmetalated products with Pt(II) and Hg(II) cations.^{4,5} In an attempt to study the ligation behavior of chalcogenaza macrocycles, we are now interested in the coordination behavior of the reduced form of the Schiff base macrocycles.¹⁰ The reduced form of the macrocycle will be more flexible. Also, it has only sp³-hybridized donor atoms, and it can accommodate a larger range of shapes and sizes than the parent Schiff base macrocycle can, which has sp² hybridized donor atoms. Also, the reduced macrocycles have weaker E···N (E = Se, Te) interactions as evidenced from the multinuclear NMR spectra and single crystal structure studies.¹⁰ Herein, we are reporting the ligation property of 28-membered selenaza macrocycle **4** (C₃₆H₄₆N₆Se₂) toward Pb(II) and Hg(II), where interestingly the central metal atom is coordinated to nitrogen atoms only.



Experimental Section

All reactions were carried out under nitrogen or argon using standard vacuum-line techniques. Solvents were purified and dried by standard procedures and were freshly distilled prior to use. Ligand **4** was prepared by the reported procedure.⁶ Melting points were recorded in capillary tubes and are uncorrected. The ¹H, ¹³C, and ⁷⁷Se spectra were recorded in CD₃CN on a Varian VXR 300S spectrometer or a 500 MHz Bruker spectrometer. Chemical shift data were referenced to internal TMS (¹H, ¹³C) or external Me₂Se₂ (⁷⁷Se). Elemental analysis was performed on Carlo-Erba model 1106 and Eager 300 EA1112 elemental analyzers. The IR spectra were recorded as KBr pellets on a Thermo Nicolet Avatar 320 FTIR spectrometer. The ESI MS mass spectra were recorded at room temperature on a Q-ToF micro (YA-105) mass spectrometer.

Synthesis of [Hg₂(PF₆)₂{C₃₆H₄₆N₆Se₂}] (5**).** To the methanol solution (20 cm⁻³) of the ligand (0.3 g, 0.41 mmol) was added Hg(OCOCH₃)₂ in a 1:1 or 1:2 equivalent ligand to metal salt ratio. After refluxing for half an hour, the reaction mixture was filtered.

To the filtrate was added an excess of NH₄PF₆. Cooling of the hot reaction mixture at room temperature afforded the complex as white crystals which were washed with methanol and vacuum dried. Yield: 0.14 g, 24%. Mp: 160 °C(d). Anal. Calcd for C₃₆H₄₆N₆Se₂Hg₂P₂F₁₂: C, 30.63; H, 3.28; N 5.95. Found: C, 32.77; H, 3.67; N, 6.31. IR (KBr) (cm⁻¹): 3657, 3322, 3056, 1463, 1438, 842, 557. ESI MS: found 1320.5, 1269.5, 1067.4, 921.4, 719.4; calcd for [4 + 2Hg + PF₆ + CH₃CN] m/e = 1320, [4 + 2Hg + PF₆] m/e = 1265, [4 + Hg] m/e = 919, [4] = 719. ¹H NMR (300 MHz, CD₃CN, 25 °C): complex pattern. ¹³C NMR (δ 300 MHz, CD₃CN, 25 °C): 140.8, 136.7, 136.7, 132.6, 132.2, 130.8, 130.5 for aromatic carbon atoms, 54.7 (Ar-CH₂), 48.6 (CH₂), 46.8 (CH₂). ⁷⁷Se NMR (300 MHz, CD₃CN, 25 °C): 336 and 339 ppm.

Synthesis of [Pb₂(PF₆)₂(OCOCH₃)₂{C₃₆H₄₆N₆Se₂}]·2CH₃CN (6**).** To the methanol solution (20 cm⁻³) of the ligand (0.3 g, 0.41 mmol) was added Pb(OCOCH₃)₂·4H₂O in a 1:1 or 1:2 equivalent ligand to metal salt ratio. After refluxing for half an hour, the reaction mixture was filtered. To the filtrate was added an excess of NH₄PF₆. The complex was separated as white powder, which was repeatedly recrystallized by slow ether diffusion into the CH₃CN solution of the complex. Yield: 0.26 g, 39%. Mp 235–237 °C. Anal. Calcd for C₄₄H₅₇N₈Se₂Pb₂P₂F₁₂O₄: C, 32.54; H, 3.53; N, 6.89. Found: C, 26.44; H, 2.91; N, 4.18. IR (KBr) (cm⁻¹): 3638s, 3280b, 2354, 1552s, 841b, 558s. MS (ESI MS): found, 1399, 1055, 987; calcd for [4 + 2Pb + 2CH₃COO + PF₆] m/e = 1400, [4 + Pb + 2CH₃COO] m/e = 1055, [4 + Pb + CH₃COO] m/e = 985. ¹H NMR (400 MHz, CD₃CN, 25 °C): complex pattern. ¹³C NMR (δ 400 MHz, CD₃CN, 25 °C): 139.3, 134.8, 131.4, 131.2, 129.8, 128.9 for aromatic carbon atoms, 52.1 (Ar-CH₂), 50.4 (CH₂), 47.1 (CH₂), 179.6 (C=O), 25.5 (CH₃). ⁷⁷Se NMR (500 MHz, CD₃CN, 25 °C): 317.1 and 317.9 ppm.

X-ray Crystallography. The diffraction measurements for complexes were performed at room temperature on a Bruker SMART diffractometer with graphite-monochromated Mo Kα radiation (λ = 0.71073 Å). The data were corrected for Lorentz, polarization, and absorption effects. The structures were determined by routine heavy-atom methods using SHELXS 97¹¹ and Fourier methods and refined by full-matrix least squares with the non-hydrogen atoms anisotropic and hydrogen with fixed isotropic thermal parameters of 0.07 Å² by means of the SHELEXL 97¹² program. The hydrogens were partially located from difference electron-density maps, and the rest were fixed at predetermined positions. Scattering factors were from common sources.¹³ Some details of the data collection and refinement are given in Table 1.

Results and Discussion

Refluxing Hg(OCOCH₃)₂ with ligand **4** in MeOH followed by the addition of NH₄PF₆ afforded white crystals of [Hg₂(PF₆)₂{C₃₆H₄₆N₆Se₂}] (**5**) (Scheme 1). Attempted synthesis of complex **5** using mercurous chloride or mercuric chloride produced black and white products, respectively, which were difficult to characterize due to the solubility problems. Also, the complexation reaction with mercurous acetate afforded a mixture of products. Complex **5** is insoluble in most of the organic solvents and only partially soluble in CH₃CN.

Its elemental analysis did not give satisfactory data even after repeated crystallization, and this may be due to improper

- (4) Menon, S. C.; Singh, H. B.; Patel, R. P.; Kulshreshtha, S. K. *J. Chem. Soc., Dalton. Trans.* **1996**, 1203.
- (5) Menon, S. C.; Panda, A.; Singh, H. B.; Butcher, R. J. *Chem. Commun.* **2000**, 143.
- (6) Panda, A.; Menon, S. C.; Singh, H. B.; Butcher, R. J. *J. Organomet. Chem.* **2001**, 623, 87.
- (7) Panda, S.; Singh, H. B.; Butcher, R. J. *Chem. Commun.* **2004**, 322.
- (8) Menon, S. C.; Panda, A.; Singh, H. B.; Patel, R. P.; Kulshreshtha, S. K.; Darby, W. L.; Butcher, R. J. *J. Organomet. Chem.* **2004**, 1452.
- (9) Panda, A.; Menon, S. C.; Singh, H. B.; Morley, C. P.; Bachman, R.; Cocker, T. M.; Butcher, R. J. Unpublished work.
- (10) Panda, S.; Singh, H. B.; Butcher, R. J. Unpublished work.

- (11) Sheldrick, G. M. *SHELXS 97, Program for the Solution of Crystal Structures*; University of Göttingen: Göttingen, Germany, 1990.
- (12) Sheldrick, G. M. *SHELXL 97, Program for Refining Crystal Structures*; University of Göttingen: Göttingen, Germany, 1997.
- (13) *International Tables for X-ray Crystallography*; Kynoch Press: Birmingham, U.K., 1974; Vol. 1, pp 99 and 149.

Table 1. Crystallographic Data for [Hg₂(PF₆)₂{C₃₆H₄₆N₆Se₂}] (**5**) and [Pb₂(PF₆)₂(OCOCH₃)₂{C₃₆H₄₆N₆Se₂}](CH₃CN)₂ (**6**)

	5	6
empirical formula	C ₃₆ H ₄₆ F ₁₂ - Hg ₂ N ₆ P ₂ Se ₂	C ₄₄ H ₅₇ F ₁₂ N ₈ - O ₄ P ₂ Pb ₂ Se ₂
color	colorless	colorless
fw	1407.80	1624.22
cryst syst	triclinic	triclinic
space group	<i>P</i> $\bar{1}$	<i>P</i> $\bar{1}$
<i>a</i> (Å)	9.5106(5)	9.4668(5)
<i>b</i> (Å)	11.5222(6)	11.9937(6)
<i>c</i> (Å)	11.8161(6)	25.2319(14)
α (deg)	115.6110(10)	102.4130(10)
β (deg)	96.5190(10)	97.6130(10)
γ (deg)	106.2910(10)	94.8540(10)
<i>V</i> (Å ³)	1078.72(10)	2754.3(3)
<i>Z</i>	1	2
temp (K)	293(2)	103(2)
abs coeff (mm ⁻¹)	8.957	7.573
obsd reflns [<i>I</i> > 2 σ]	5132	11150
final <i>R</i> (<i>F</i>) [<i>I</i> > 2 σ] ^a	0.0560	0.0324
w <i>R</i> (<i>F</i> ²) indices [<i>I</i> > 2 σ]	0.1519	0.0708

^a Definition: $R(F_o) = \sum ||F_o| - |F_c|| / \sum |F_o|$ and $wR(F_o^2) = \{ \sum [w(F_o^2 - F_c^2)^2] / \sum [w(F_c^2)^2] \}^{1/2}$.

combustion of the heavy metal complex during analysis.¹⁴ The X-ray powder diffraction has been done to find out the bulk composition of the sample. The matching of the simulated pattern from the single crystal data (Supporting Information) and XRPD pattern proves the presence of a single product in the bulk sample. The ESI MS recorded in acetonitrile indicated the ligand complexation with two mercury cations. Though the molecular ion peak was not observed in the mass spectroscopic condition, there were peaks at *m/z* 1320 for [**4** + 2Hg + PF₆ + CH₃CN], and the peak at *m/z* 1269 was for [**4** + 2Hg + PF₆]. The IR spectrum of the complex shows NH stretching at 3322 as a broad multiplet and NH bending at 1585 cm⁻¹, indicating nitrogen coordination to the metal atom. The strong peaks at 842 and 557 cm⁻¹ indicate the presence of PF₆⁻ anion. The crystallographic data (vide infra) showed the presence of a mercurous cation trapped inside the cavity of the macrocycle. Most of the known mercury complexes of macrocycles have a formal +2 oxidation state, and Hg₂²⁺ complexes with macrocycle are relatively scarce.^{15–17} Catalano et al. have reported the crystal structure of a mercurous cation trapped inside a metallocryptand.¹⁵ Peringer et al. reported a mercurous complex sandwiched by two crown ethers.¹⁶ Yordanov et al. reported the extraction of Hg₂²⁺ by calixarene.¹⁷ Complex **5** is the first example of a structurally characterized mercurous cation complex of a monocycle where Hg₂²⁺ is trapped inside the cavity of the monocycle. Catalano et al. have explained why the formation of mercurous ion may be due to presence of HgO impurity with Hg(0) and the reaction of Hg(II) and Hg(0) strongly favors Hg₂²⁺.^{15,18} Recently, Baldwin et al. have reported the formation of mercurous

dimer from the mercuric salt.¹⁹ They have also explained it as the disproportion of Hg(II) and Hg(0) to give Hg₂²⁺.

The ¹H NMR spectrum of **5** shows a complex pattern as well as broadening of the peaks. The complex nature of the spectrum was further investigated by recording variable temperature NMR at lower temperature. Upon lowering the temperature from 25 to 0 °C, there is slight splitting of the peaks observed; however, these start broadening again at –20 °C (Figure 1).

This broadening of the peaks may be due to the dynamic process occurring in the solution of the complex. The ¹³C NMR spectrum shows the expected number of peaks and proves the existence of a single species in the solution state. The ⁷⁷Se NMR shows two closely spaced peaks at 336 and 339 ppm of unequal intensity, which may be explained in terms of the presence of different Se containing species in the solution state.²⁰ There is only a marginal shift in the chemical shift value as compared to the free ligand (328 ppm) indicating no coordination of any of the Se atoms to Hg₂²⁺ in the solution state.

The molecular structure of the complex is presented in Figure 2. The selected bond distances and angles are given in Table 2. The molecule is centrosymmetric, and only half of the molecule represents the asymmetric unit. The structure shows a rare example of a Hg₂²⁺ cation trapped inside the macrocycle, bonded through 6 nitrogen atoms. The Hg–Hg#1 distance is 2.5358(8) Å and is much shorter than Hg–Hg distance of 3.00 Å in solid mercury and also shorter than the sum of the covalent radii, 2.88 Å. This distance is shorter than the Hg–Hg distance of 2.7362(6), 2.6881(4), and 2.5469(8) Å reported in [Pt₂Hg₂(P₂phen)₃](PF₆)₂, [Pd₂Hg₂(P₂phen)₃](PF₆)₂, and [Hg₂(TLA)₂](CLO₄)₂ (TLA is abbreviation for tris[(2-(6-methylpyridyl)methyl]amine) complexes, respectively;^{15,19} however, it is comparable to the Hg–Hg distance in Hg₂Cl₂, 2.53 Å.²¹ The Hg–Hg bond distance is near the higher end of the 2.49–2.56 Å range reported for the mercurous ion complexes.¹⁵ The nitrogen atoms around the mercurous cation are arranged in an antiprismatic manner. The Hg–N(2A) 2.342(8) Å, Hg–N(1B)#1 2.468(8) Å, and Hg–N(1A) 2.503(8) Å distances are greater than the sum of covalent radii of Hg (1.49 Å) and N (0.75 Å), but are, however, smaller than the sum of the van der Waals radii (3.1 Å). The Hg–N distances are longer than the Hg–N (amine) distances reported for [Hg₂(TLA)₂](CLO₄)₂ (2.297–(6) Å). This lengthening of the Hg–N may be rationalized in terms of the following: (a) the TLA ligand is an acyclic ligand and thus is more flexible where the amine nitrogen can come closer to the metal center. (b) In our case, the ligand is cyclic, and steric requirement of the metal ion forces

(14) It is possible that the bulk sample contains trace quantities of impurities even after repeated recrystallization.

(15) Catalano, V. J.; Malwitz, M. A. *Inorg. Chem.* **2002**, *41*, 6553.

(16) Malleier, R.; Kopacka, H.; Schuh, W.; Wurst, K.; Peringer, P. *Chem. Commun.* **2001**, 51.

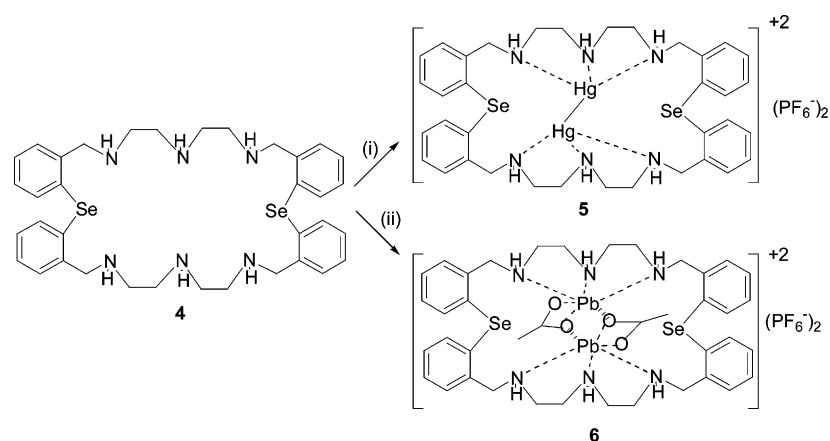
(17) Yordanov, A. T.; Roundhill, D. M.; Mague, J. T. *Inorg. Chim. Acta* **1996**, *250*, 295.

(18) Greenwood, N. N.; Earnshaw, A. *Chemistry of the Elements*; Pergamon Press: Oxford, 1994.

(19) Bebout, D. C.; Bush, J. F., II; Shumann, E. M.; Viehweg, J. A.; Kastner, M. E.; Parrish, D. A.; Baldwin, S. M. *J. Chem. Crystallogr.* **2003**, *33*, 457 and references therein.

(20) The nonequivalence of ⁷⁷Se NMR intensities for the two peaks could be due to the presence of several asymmetric nitrogens, which can give rise to diastereomers. Although the metal ions are normally labile, the possibility of the presence of diastereomers “frozen” on the NMR time scale cannot be ruled out.

(21) Boldersen, K.; Hummel, H.-U. *Mercury in Comprehensive Coordination Chemistry*; Wilkinson, G., Gillard, R. D., McCleverty, J. A., Eds.; Pergamon Press: Oxford, 1987; Vol. 5, p 1047.

Scheme 1^a

^aReagents and conditions: MeOH, (i) Hg(OCOCH₃)₂, NH₄PF₆; (ii) Pb(OCOCH₃)₂·4H₂O, NH₄PF₆.

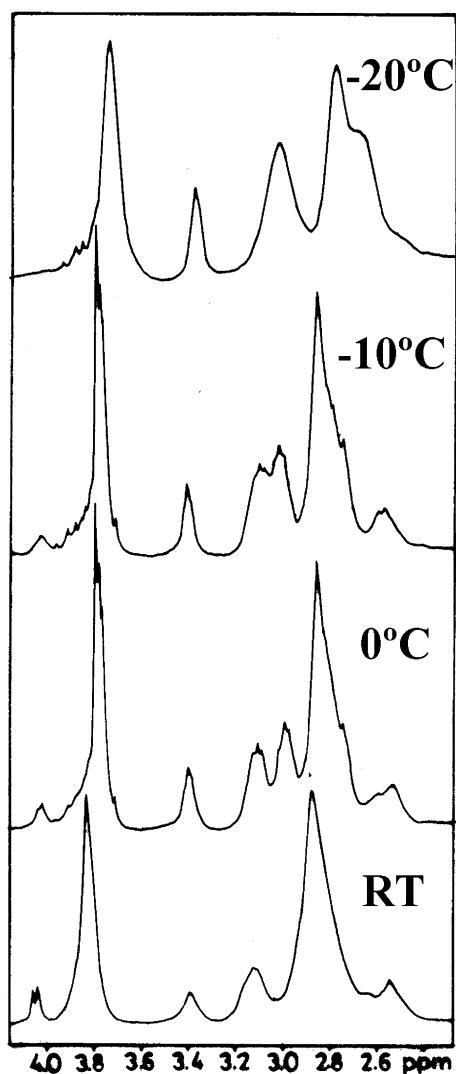


Figure 1. Parts of the 300 MHz ¹H NMR spectra of **5** recorded in CH₃CN-*d*₃ at different temperatures.

the ligand into a highly puckered conformation. This may lead to a longer Hg–N bond length. (c) Also, the N atom in TLA ligand is sp² hybridized whereas the N atom in complex **5** is sp³ hybridized resulting in the shortening of the Hg–N bond distance in TLA and lengthening of the Hg–N bond

distance in **5**. The transannular Se···Se distance (11.1962 Å) is longer than the Se···Se distance in the parent Schiff base macrocycle **3** (C₃₆H₃₈N₆Se₂).⁶ The nearest Se···Hg distance is 5.6601 Å, and the other Se···Hg#1 distance is 5.8185 Å. These distances are more than the sum of the van der Waals radii of Se and Hg and indicate that there is no interaction between Hg and Se in the solid state. As mercury is a soft acid and Se is a soft donor site, it was expected that there would be an interaction between Se and Hg.²² We have recently reported some Pd(II) complexes of the 22-membered selenaza/telluraza macrocycles.⁷ The structure of the Pd(II) complex of the 22-membered selenaza macrocycle shows coordination of Pd(II) to only hard N donor atoms. This is in contrast to the isolation of Pd(II) complexes of mixed donor Se/Te macrocycles containing O or P where Pd(II) coordinates to soft donor centers Se/Te.²³ This anomalous behavior may be due to the formation of stable 5-membered chelate rings rather than the formation of six-membered chelate rings which would result on coordination to Se. However, the molecular structure of the Pd(II) complex of the corresponding 22-membered telluraza macrocycle shows coordination to two nitrogen and two tellurium atoms.⁷ The coordination of Te to Pd(II) may be due to the greater σ-donor property of the Te over Se leading to soft–soft interaction and stabilization of the six-membered chelate ring. Thus, the unusual noninteraction between Hg and Se in this case results from the conformational requirement of the ligand around the central Hg(I) for coordination with donor atoms as well as the chelate ring effect.

Reaction of **4** with either 1 or 2 equiv of Pb(CH₃COO)₂·4H₂O in refluxing methanol solution afforded complex **6** as a white solid. The complex is insoluble in common chlorinated solvents and hydrocarbons; however, it is soluble in MeCN, MeNO₂, acetone, DMF, and DMSO. Slow diffusion of ether into the MeCN solution of **6** afforded white crystals

- (22) Mazouz, A.; Meunier, P.; Kubicki, M. M.; Hanquet, B.; Amardeil, R.; Bornet, C.; Zahidi, A. *J. Chem. Soc., Dalton Trans.* **1997**, 1043.
 (23) (a) Bornet, C.; Amardeil, R.; Meunier, P.; Daran, J. C. *J. Chem. Soc., Dalton Trans.* **1999**, 1039. (b) Li, J. L.; Meng, J. B.; Wang, Y. M.; Wang, J. T.; Matsuura, T. *J. Chem. Soc., Perkin Trans. 1* **2001**, 1140. (c) Hesford, M. J.; Levason, W.; Matthews, M. L.; Orchard S. D.; Reid, G. *Dalton Trans.* **2003**, 2434. (d) Hesford, M. J.; Levason, W.; Matthews M. L.; Reid, G. *Dalton Trans.* **2003**, 2852.

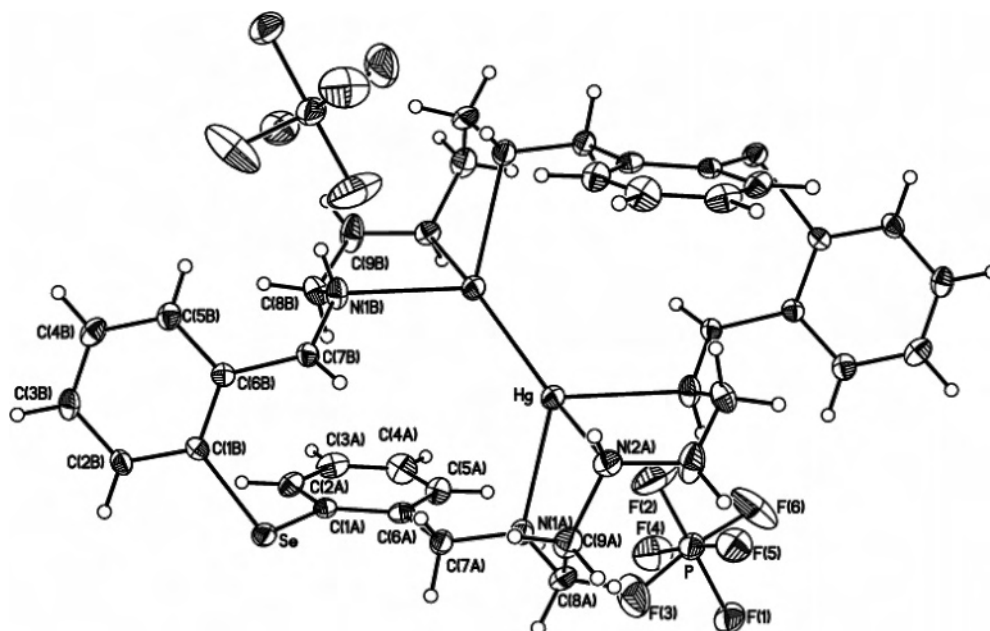


Figure 2. ORTEP diagram of complex **5** cation.

Table 2. Selected Bond Lengths (Å) and Angles (deg) for **5**

Hg–N(2A)	2.342(8)	Hg–N(1B)#1	2.468(8)
Hg–N(1A)	2.503(8)	Hg–Hg#1	2.5358(8)
Se–C(1B)	1.926(9)	Se–C(1A)	1.928(9)
N(2A)–Hg–N(1B)#1	74.3(3)	N(2A)–Hg–N(1A)	74.5(3)
N(1B)#1–Hg–N(1A)	104.4(3)	N(2A)–Hg–Hg#1	143.4(2)
N(1B)#1–Hg–Hg#1	119.4(2)	N(1A)–Hg–Hg#1	126.47(18)
C(1B)–Se–C(1A)	99.6(3)		

of the complex. The complex crystallizes with two molecules of the solvent (*vide infra*). The elemental analysis did not give satisfactory data even after repeated purifications, although they were reproducible for samples prepared in different batches. This may be due to improper combustion of the complex due to the presence of heavy metal during analysis.¹⁴ The bulk sample was not sufficiently crystalline enough for satisfactory XRPD analysis. The ESI MS shows the highest peak at $m/e = 1399$, which corresponds to $[4 + 2\text{Pb} + 2\text{CH}_3\text{COO} + \text{PF}_6]$. The formation of the binuclear complex even when the metal-to-ligand ratio was 1:1 may be due to the cooperative effect of complex formation. The IR spectrum of the complex shows peaks consistent with the highly coordinated carboxylic group with stretching frequency at 1552 cm^{-1} as an intense sharp peak. The peaks at 841 and 558 cm^{-1} indicate the presence of PF_6 anion. The peak at 2354 cm^{-1} in the IR spectrum confirms the presence of CH_3CN in the molecule. The ^1H NMR spectrum of the **5** is also complex, and the peaks are broad. This may be due to some dynamic process occurring in the solution. However, the ^{13}C NMR spectrum shows the expected number of peaks for the complex and confirms the presence of a single species in the solution. The peaks at 25 and 179 ppm indicate the presence of chelating acetate ion. The ^{77}Se NMR shows two very closely spaced doublets at 317.1 and 317.9 ppm (free ligand 328 ppm) indicating that there is no interaction between Pb and Se in the solution state and that there are more than one Se containing species present.²⁰

An ORTEP view of **6** is shown in Figure 3. The selected bond lengths and bond angles are given in Table 3. The structure of the complex consists of a $[\text{Pb}_2(\text{OCOCH}_3)_2\text{-}\{\text{C}_{36}\text{H}_{46}\text{N}_6\text{Se}_2\}]^{+2}$ cation and PF_6^- anions. The asymmetric unit comprises two crystallographically independent molecules AB and A'B', and the unit cell contains two molecules. Each molecule in the asymmetric unit is centrosymmetric in itself. There is only little difference in bond lengths and bond angles between the two asymmetric units. The geometry around each Pb(II) is a distorted octahedron due to a stereochemically active lone pair on Pb^{2+} . The two metal atoms and the bridging oxygen atoms form a central four-membered Pb_2O_2 ring. Each acetate ion in the molecular unit acts as chelating ligand toward one metal atom and is bridging between the two metals through one of its oxygen atoms. This is the first example of a binuclear lead complex of a monocycle where the two lead atoms as well the chelating acetate anions are wrapped by the macrocycle cavity. Each Pb atom in the two molecules coordinates to 3 nitrogen atoms [Pb(1)–N(2A) $2.534(5)\text{ Å}$, Pb(1)–N(1B)#1 $2.592(5)\text{ Å}$, Pb(1)–N(1A) $2.623(5)\text{ Å}$] and [Pb(2)–N(2C) $2.495(5)\text{ Å}$, Pb(2)–N(1C) $2.604(5)\text{ Å}$, Pb(2)–N(1D)#2 $2.626(5)\text{ Å}$]. These distances are greater than the sum of covalent radii of Pb and N; however, they are smaller than the sum of van der Waals radii and are typical of reported binuclear Pb–N distances.²⁴ The Pb–O bond distances [$2.440(4)$, $2.598(4)$, $2.344(4)$, $2.693(4)$, 2.885 , 2.832 Å] are well within the van der Waals distances and are at par with the reported Pb–O distance in acetate chelating group in $[\{\text{Pb}(1,4,7\text{-tris}(\text{pyrazol-1-ylmethyl})\text{-}1,4,7\text{-triazacyclononane})\text{-}$

(24) (a) Datta, B.; Adhikary, B.; Bag, P.; Flörke, U.; Nag, K. *J. Chem. Soc., Dalton Trans.* **2002**, 2760. (b) Tei, L.; Blake, A. J.; Bencini, A.; Valtancoli, B.; Wilson, C.; Schröder, M. *Inorg. Chim. Acta* **2002**, 337, 59. (c) Bazzicalupi, C.; Bencini, A.; Fusi, V.; Giorgi, C.; Paoletti, P.; Valtancoli, B. *J. Chem. Soc., Dalton Trans.* **1999**, 393. (d) Tadokoro, M.; Sakiyama, H.; Matsumoto, N.; Okawa, H.; Kida, S. *Bull. Chem. Soc. Jpn.* **1990**, 63, 3337. (e) Tandon, S. S.; McKee, V. *J. Chem. Soc., Dalton Trans.* **1989**, 19.

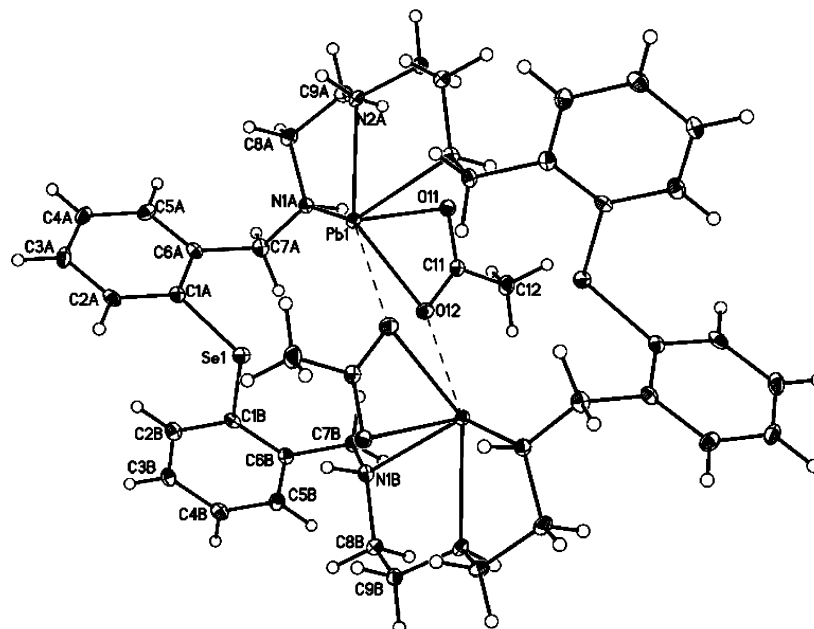


Figure 3. ORTEP diagram of complex **6** cation.

Table 3. Selected Bond Lengths (Å) and Angles (deg) for **6**

Pb(1)–N(2A)	2.534(4)	Pb(1)–N(1B)#1	2.592(4)
Pb(1)–N(1A)	2.624(4)	Pb(1)–O(11)	2.440(4)
Pb(1)–O(12)	2.598(4)		
O(11)–Pb(1)–N(2A)	74.12(13)	O(11)–Pb(1)–N(1B)#1	171.09(12)
N(2A)–Pb(1)–N(1B)#1	69.18(14)	O(11)–Pb(1)–O(12)	51.39(12)
N(2A)–Pb(1)–O(12)	124.50(13)	N(1B)#1–Pb(1)–O(12)	98.50(13)

(O₂CMe)₂][BPh₄]₂.²⁵ In one of the asymmetric units, the Pb···Se distance is 3.598 Å, which may be due to the geometrical requirement of the molecule. The Pb(1)···Pb(1) distance in the AB molecule is 4.481 Å whereas that in A'B' molecule is 4.533 Å. The distance between Se···Se in AB molecule is 7.17 Å whereas that in A'B' molecule is 9.976 Å. The distances between Pb···Pb and Se···Se show that there is no interaction between them. It is interesting to note that the corresponding Pb(II) complexation with the azathia macrocycle shows Pb(II) coordination to both S and N atoms.²⁶

Conclusions

The first example of a mercurous cation located inside a single monocycle has been structurally characterized. Mo-

lecular structure of the mercurous complex **5**, surprisingly, shows that there is no soft–soft interaction between mercury and the selenium donor atom. This particular complex demonstrates that the HSAB principle also depends on the geometrical arrangement of donor atoms in the ligand. Also, in complex **6** there is absence of Pb···Se interaction; however, one observed weak interaction between the Pb and Se may be due to the geometrical placement of the selenium around the metal. This noninteraction between the Se donor atoms and the metal atoms in the cases of both the complexes may be explained in terms of the conformational requirement of the ligand around the metal. In general, the 28-membered diselenahexaaza macrocycle may have potential use as an effective binuclear chelating ligand for toxic heavy metals such as Hg and Pb.

Acknowledgment. We would like to thank one of the referees for helpful suggestions. We are also grateful to the Department of Science and Technology (DST), New Delhi, for funding this work.

Supporting Information Available: IR and ¹³C and ⁷⁷Se NMR spectroscopic data and X-ray crystallographic data in CIF format for the structure of compounds **5** and **6**. XRPD pattern and simulated pattern from the single crystal X-ray data of complex **5**. This material is available free of charge via the Internet at <http://pubs.acs.org>.

IC0351949

(25) Vaira, M. D.; Guerra, M.; Manni, F.; Stoppioni, P. *J. Chem. Soc., Dalton Trans.* **1996**, 1173.

(26) Bashall, A.; McPartlin, M.; Murphy, B. P.; Powell, H. R.; Waikar, S. *J. Chem. Soc., Dalton Trans.* **1994**, 1383.